Bioorganic & Medicinal Chemistry 16 (2008) 9040–9049

Contents lists available at ScienceDirect

Bioorganic & Medicinal Chemistry

journal homepage: www.elsevier.com/locate/bmc

Novel naphthoquinone and quinolinedione inhibitors of CDC25 phosphatase activity with antiproliferative properties

Emmanuelle Braud [a,b], Mary-Lorène Goddard [a,b], Stéphanie Kolb [a,b], Marie-Priscille Brun [a,b], Odile Mondésert [c], Muriel Quaranta [c], Nohad Gresh [a,b], Bernard Ducommun [c], Christiane Garbay [a,b,*]

[a] Université Paris Descartes, UFR biomédicale, Laboratoire de Pharmacochimie Moléculaire et Cellulaire, 45 rue des Saints-Pères, Paris F-75006, France
[b] INSERM U648, Paris F-75006, France
[c] Université Paul Sabatier, Laboratoire de Biologie Cellulaire et Moléculaire du Contrôle de la Prolifération, UMR 5088-IFR109, Route de Narbonne, Toulouse, F-31062, France

ARTICLE INFO

Article history:
Received 5 May 2008
Revised 29 July 2008
Accepted 4 August 2008
Available online 7 August 2008

Keywords:
Cancer
Phosphatase CDC25
Cell cycle regulation
Quinone derivatives

ABSTRACT

CDC25 phosphatases are considered as attractive targets for anti-cancer therapy. To date, quinone derivatives are among the most potent inhibitors of CDC25 phosphatase activity. We present in this paper the synthesis and the biological evaluation of new quinolinedione and naphthoquinone derivatives, containing carboxylic or malonic acids groups introduced to mimic the role of the phosphate moieties of Cyclin-Dependent Kinase complexes. The most efficient compounds show inhibitory activity against CDC25B with IC_{50} values in the 10 μM range, and are cytotoxic against HeLa cells.

1. Introduction

CDC25 dual-specificity phosphatases are major actors of eukaryotic cell cycle regulation and are involved in essential cellular events such as growth, division, or replication. They thus activate Cyclin-Dependent Kinase (CDK) complexes by dephosphorylating two adjacent threonine and tyrosine residues allowing progression of the cell cycle.[1,2]

The human genome encodes three CDC25 homologues, namely CDC25A, B, and C.[3–5] Though their entire role has not been elucidated yet, these three isoforms have been shown to play multiple roles and to cooperate at various stages of the cell cycle. CDC25A has been demonstrated to activate CDK2/cyclin E and CDK2/cyclin A complexes allowing progression into S phase[6–8] and is also involved at mitosis in the control of CDK1/cyclin B.[9] Isoform B catalyzes the dephosphorylation of CDK1/cyclin A to drive the cell through the G2/M transition[10] and has also been shown to play a role in centrosome duplication and in S-phase.[11,12] CDC25B expression is also required for checkpoint recovery after DNA repair.[13,14] CDC25 C is involved in cell progression in mitosis due to its ability to activate CDK1/cyclin B complex[15] and might also be involved in the control of S-phase.[16]

Overexpression of CDC25A and B was observed in a wide variety of tumors and related cancer cell lines including prostate, breast, or gastric cancers, hepatocarcinomas and non-hodgkinian lymphomas.[9,17] Such an abnormal expression often correlates with poor prognosis and since isoforms A and B possess oncogenic properties,[18] CDC25 phosphatases are now considered as particularly attractive targets toward novel approach in cancer treatment.[9]

Several classes of inhibitors have been described so far (for recent reviews, see Boutros et al.[9] and Contour-Galcera et al.[19]). The most potent ones share the para-quinone moiety such as the thio-ether derivative Cpd 5 that inhibits CDC25 activity in Hep3B cells[20,21] or NSC 95397 that blocks cell cycle at the G2/M transition.[22] Among the quinolinedione derivatives, NSC 663284 inhibits CDC25 activity in an irreversible manner by binding covalently to a serine residue.[23,24] Adociaquinone B is a natural product isolated from a marine sponge that inhibits in vitro CDC25B activity with an IC_{50} value of 70 nM.[25] More recently, BN82685 was demonstrated to inhibit in vivo the growth of human pancreatic MiaPaCa2 tumors xenografted on athymic nude mice.[26,27] IRC-083864 containing two quinone nuclei is the most potent CDC25 inhibitor that also exhibits antiproliferative properties against MiaPaCa2 and LNCaP cell lines and xenografted tumors.(Chart 1) [28]

We have previously reported the synthesis and the inhibitory activity of several naphthoquinone derivatives containing carboxylate groups designed to interact with CDC25B through arginine residues R482 and R544 involved in the recognition of the CDKs (Chart 2).[29] These inhibitors displayed anti-CDC25 activity with IC_{50} values in the micromolar range as well as anti-proliferative properties toward HeLa cells. They also caused hyperphosphorylation of CDK1

* Corresponding author. Tel.: +33 142 864 080; fax: +33 142 864 082.
E-mail address: christiane.garbay@univ-paris5.fr (C. Garbay).

0968-0896/$ - see front matter © 2008 Published by Elsevier Ltd.
doi:10.1016/j.bmc.2008.08.009

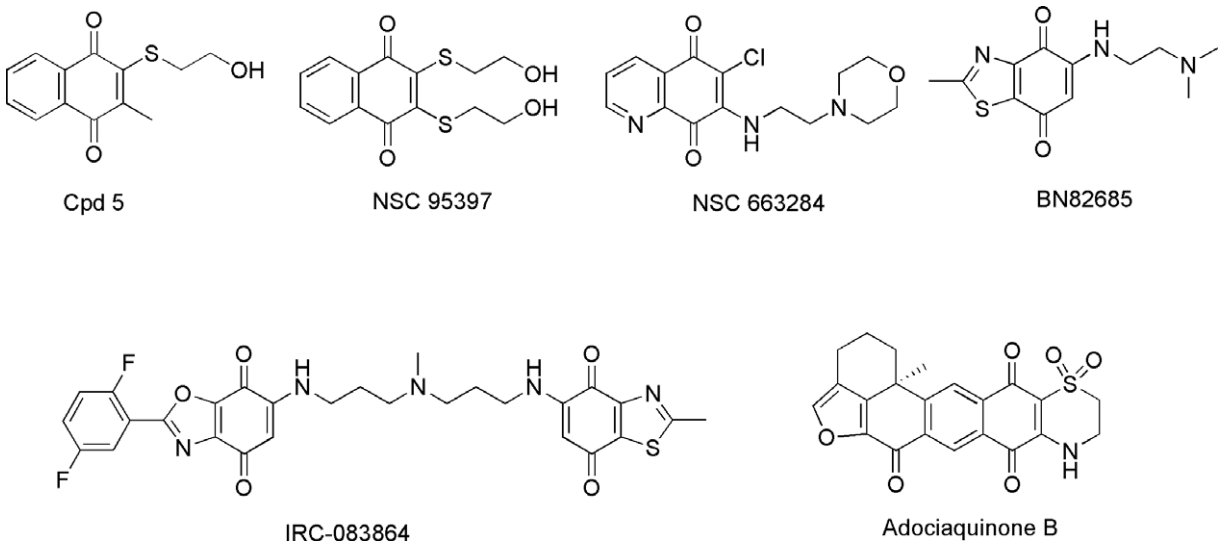

Chart 1. Structures of CDC25 phosphatase inhibitors.

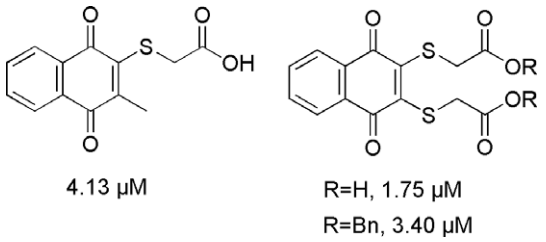

Chart 2. CDC25 inhibitors designed to interact with the phosphate binding pocket.

showing that they were actually targeting CDC25 in HeLa cells. In order to improve the potency of these compounds, we have developed new series of naphthoquinone and quinolinedione derivatives by introducing a malonic acid group at the extremity of an aliphatic side chain to optimize interactions between the carboxylate groups and the arginine residues.

2. Chemistry

Naphthoquinones **1e** and **2e** were prepared following a three-step procedure using the commercially available 2-bromomethylnaphthalene **1** or 2-(2-naphthyl)ethyl bromide **2** which was obtained by bromination of naphthaleneethanol (Scheme 1) as starting material.[30] Bromide derivatives **1** and **2** were converted into the corresponding dibenzyl or diterbutyl malonate analogues **1a,b**–**2a,b** using the malonic synthesis conditions with yields ranging from 80% to 89%. The naphthalene derivatives **1a,b**–**2a,b** were then oxidized by a mixture of periodic acid and chromic anhydride into 1,4-naphthoquinone derivatives **1c,d**–**2c,d** with low to moderate yields (15–39%).[31] The diterbutyl malonates **1d** and **2d** were hydrolyzed using trifluoroacetic acid in dichloromethane to provide the corresponding malonic acids **1e** and **2e** in 70% and 82% yields, respectively.

Compound **3** was obtained in 13% yield following the protocol described by Salmon-Chemin and co-workers by reacting menadione and glutaric acid in the presence of silver nitrate as a catalyst and ammonium salt (Scheme 2).[32]

Compound **4** was prepared using a 1,4-Michael type addition of mercaptopropanoic acid to 2-methyl-[1,4]-naphthoquinone in the presence of DBU in ether in 20% yield (Scheme 2).[29]

The 6,7-dibromo-5,8-quinolinedione **5** was obtained by oxidizing the commercially available 5-amino-8-hydroxyquinoline with $NaBrO_3$/HCl in 43% yield.[33] Subsequently, the 6,7-disubstituted quinoline-5,8-diones **6** and **7** were synthesized in 33% and 63% yields, respectively, using a 1,4-Michael-type addition of 2.5 equivalents of mercaptoacetic acid or mercaptopropanoic acid to **5** in the presence of triethylamine in THF at room temperature (Scheme 2).[34]

3. Results and discussion

3.1. Enzymatic activity

In a previous work, we demonstrated that naphthoquinone derivatives bearing carboxylic groups introduced to mimic the role

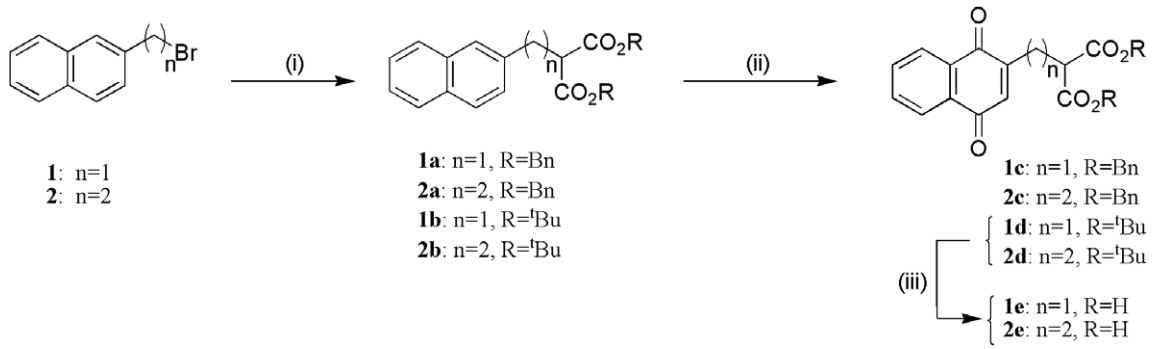

Scheme 1. Reagents and conditions: (i) NaH, $CH_2(CO_2R)_2$, DMF, rt; (ii) HIO_4, CrO_3, CH_3CN, 5 °C then rt; (iii) TFA, CH_2Cl_2, rt.

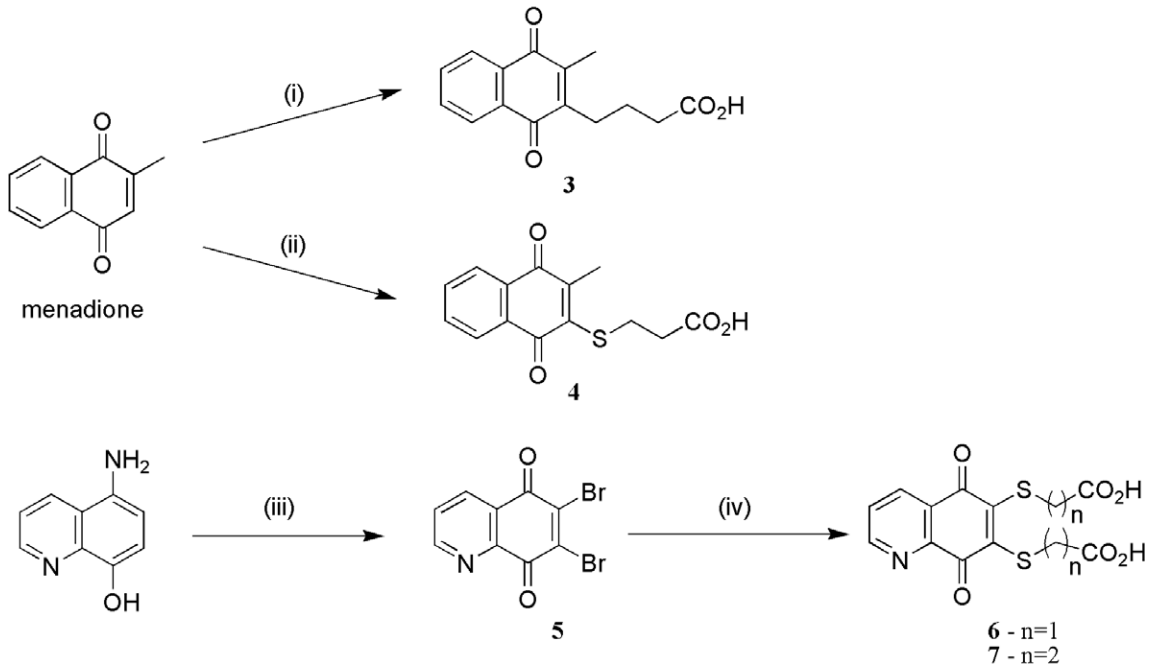

Scheme 2. Reagents and conditions: (i) $HO_2C–(CH_2)_3–CO_2H$ (3 equiv), $AgNO_3$, $(NH_4)_2S_2O_8$ (1.3 equiv), CH_3CN/H_2O (30/70), 60 °C; (ii) $HS–(CH_2)_2–CO_2H$ (1 equiv), DBU, ether, rt; (iii) $NaBrO_3$, concd HCl, 50 °C; (iv) $HS–(CH_2)_n–CO_2H$ (2.5 equiv), Et_3N, THF, rt.

of the phosphate moieties of CDKs showed CDC25 phosphatase inhibitory activity with IC_{50} values in the micromolar range.[29] Molecular dynamics calculations were performed on these carboxylic acid derivatives using the program Discover (Accelrys) and the available 3D crystal structure of CDC25B catalytic domain (PDB 1QB0) to propose a binding mode for these inhibitors. Strong ionic interactions between the carboxylate groups and arginine residues R479, R482, or R544 were observed while the naphthoquinone core was located out of the floor of the active site. In order to optimize these interactions and enhance activity, we replaced carboxylic groups by malonic acids and similar docking calculations were performed on malonic acid **1e** to examine possible interactions. These studies suggested that **1e** displayed a similar binding mode with both carboxylate groups interacting with the three arginine residues R479, R482, and R544 while the naphthoquinone core was still placed outside the active site (Fig. 1). We thus expected that this series of new malonic compounds would be most or at least as efficient as their previously reported carboxylic analogs.[29]

All our compounds were evaluated for their CDC25 inhibitory activity on an enzymatic assay using the human recombinant fused MBP-CDC25B3 protein with fluorescein 3,6-diphosphate (FDP) as the substrate (Table 1). Cpd 5 and NSC 95397 were evaluated as references in the same conditions. We previously discussed the discrepancies observed between the IC_{50} value of NSC 95397 that we measured and the one reported in the literature.[29]

In the malonic acid series, an increase of the aliphatic side-chain length was correlated with a stronger potency since compound **2c** was about fourfold more active than **1c,** and **2e** displayed a twofold stronger inhibitory activity against CDC25B than **1e**. Unexpectedly, the malonic acid derivatives **1e** and **2e** were less active than the corresponding dibenzyl esters **1c** and **2c**, **2e** inhibiting CDC25 activity with an IC_{50} value of 24.7 μM versus 10.7 μM for **2c**. These results suggest that benzyl derivatives **1c** and **2c** should adopt a different binding mode than the malonic acids **1e** and **2e**.

Replacement of the malonic group by a carboxylic moiety suppressed enzymatic activity, as compound **3** was shown to display no activity against CDC25B. Such dramatic decrease could be linked to a loss of interactions between the terminal carboxylate group and the arginine residues. Thus, in the malonic acid series, only one of the two carboxylates may be required for inhibitory activity. By contrast, introduction of a thio-alkyl side chain containing only one carboxylate group retained activity, as compound **4** was the most active derivative with an IC_{50} value of 4.55 μM. The presence of a sulfur atom that links the aliphatic side chain to the naphthoquinone core was therefore essential for activity.

Lazo et al. previously demonstrated that substitution with amino groups at positions 6 or 7 on the quinolinedione core was required for efficient CDC25 inhibition.[23] Since the presence of the thio-ether side chain is also significant for CDC25 inhibitory activity, quinolinediones **6** and **7** were accordingly synthesized. Unfortunately, neither of them led to the expected increase of potency as both compounds displayed comparable activities with IC_{50} values of 11.2 and 10 μM, respectively. The length of the alkyl side chains had no effect on the inhibitory properties.

To further investigate the effects of the thio-ether side chains, the 6,7-dibromoquinolinedione **5** was also evaluated on the enzymatic assay and exhibited an IC_{50} value of 5.3 μM. Thus, for this limited family of quinolinedione derivatives, substitution at the 6- and 7-positions with thiol groups led to a slight loss of activity. In fact, the 6,7-dibrominated quinolinedione **5** was as active as Cpd 5 and NSC 95397 in the present test. On the other hand, the analogue of compound **6** in the naphthoquinone series displayed an IC_{50} value of 1.75 μM, lower than that of **5**.[29]

We next determined the kinetic properties of CDC25 inhibition by compounds **4** and **6**. The K_m value with FDP was 2.89 ± 0.30 μM. Inhibition of CDC25B by the potent naphthoquinone **4** and quinolinedione **6** appeared to be most consistent with a mixed-competitive inhibition kinetic model (Fig. 2). This inhibition model was previously reported for NSC 95397,[22] NSC 663284[23], and also for other types of CDC25 inhibitors such as steroidal or maleic anhydrides derived inhibitors.[35,36]

Since quinone derivatives are often responsible for ROS generation, we investigated the effect of increased dithiothreitol (DTT) concentrations on the inhibitory activity of compounds **4** and **6**. Enzymatic assays were conducted as described in Section 5 replacing the normally used 1 mM DTT concentration by 10 and 20 mM.

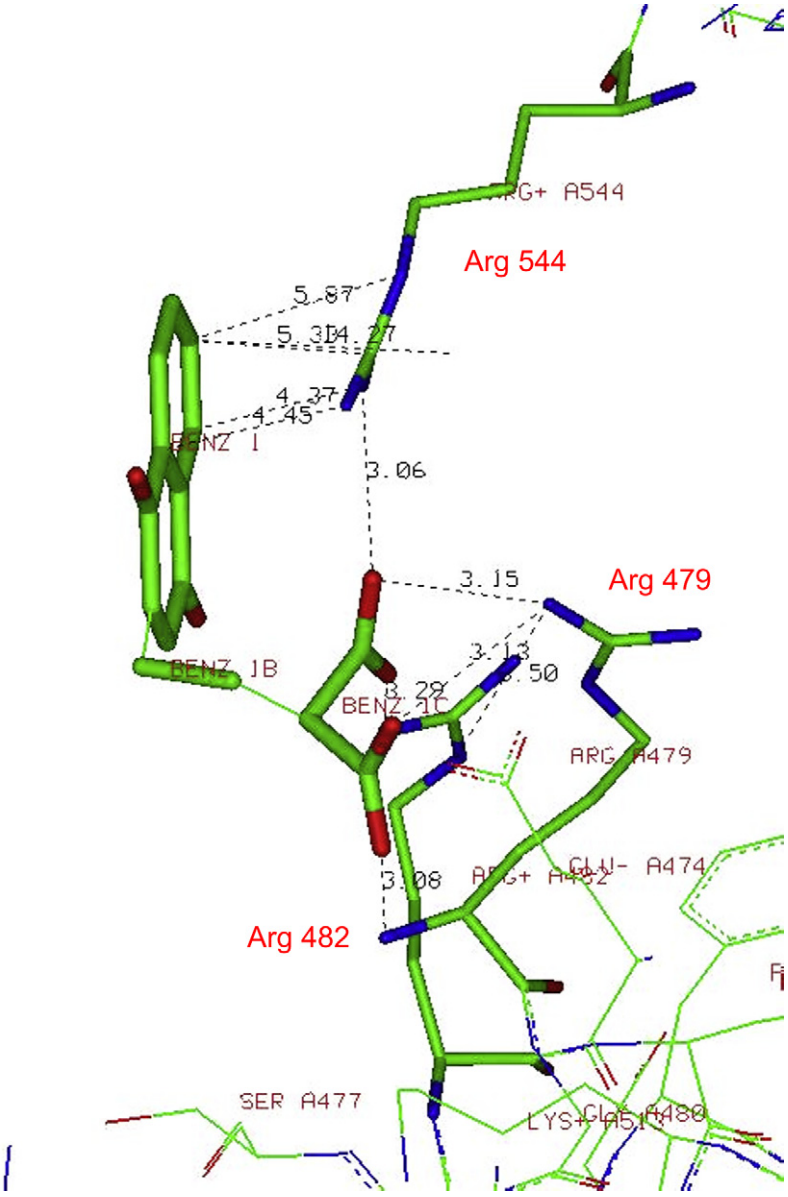

Figure 1. Molecular dynamics calculations. Docked pose of compound **1e** in CDC25B active site obtained using Discover (Accelrys).

Table 1
In vitro activity against recombinant MBP-CDC25B3 and cytotoxicity measured on HeLa cell line.

Compound	Enzymatic assay[a] IC_{50} ± SD (μM)	Cytotoxicity[b] IC_{50} ± SD (μM)
GpdS	3.65 ± 0.2	8.8 ± 3.8
NSC 95397	3.77 ± 0.9	10.8 ± 2.9
1c	37.9 ± 4.6	21.5 ± 2.3
2c	10.7 ± 0.5	12.2 ± 3.7
1e	52.7 ± 6.0	210.7 ± 13.6
2e	24.7 ± 3.0	37.7 ± 2.2
3	>100	54.2 ± 2.9
4	4.55 ± 0.16	51.3 ± 4.1
5	5.3 ± 0.3	21.5 ± 0.3
6	11.2 ± 1.2	>100
7	10.0 ± 5.5	>100

[a] Enzyme inhibition was assayed using fluorescein 3,6-diphosphate as the substrate. The IC_{50} values and the SD were calculated from at least two independent experiments with three determinations per tested concentration.

[b] Cytotoxicity was evaluated on HeLa cells using the colorimetric assay WST-1. The IC_{50} values and the SD were calculated from three independent experiments with eight determinations per tested concentration.

Results indicated that an increase of DTT concentration was correlated with an augmentation of the IC_{50} values for both compounds consistent with ROS production in vitro (Table 2). Similar observations were already reported by Cossy et al. for some quinolinedione derivatives.[37]

3.2. Cellular activity

The naphthoquinone and quinolinedione derivatives were evaluated for their cytotoxic effects on HeLa cells treated with increasing concentrations of inhibitors using the WST-1 cell viability colorimetric assay. The results are reported in Table 1 and show these compounds to be moderately cytotoxic against HeLa cells. The most active compound was the dibenzyl malonate **2c** which exhibited an IC_{50} value similar to those of Cpd 5 and NSC 95397.

In the malonic acid series, compounds with the longer aliphatic chain appeared to be the most cytotoxic ones. Benzyl malonate **1c** displayed an IC_{50} value of 21.5 μM whereas **2c** was slightly more active with an IC_{50} value of 12.2 μM. Concerning the malonic acids,

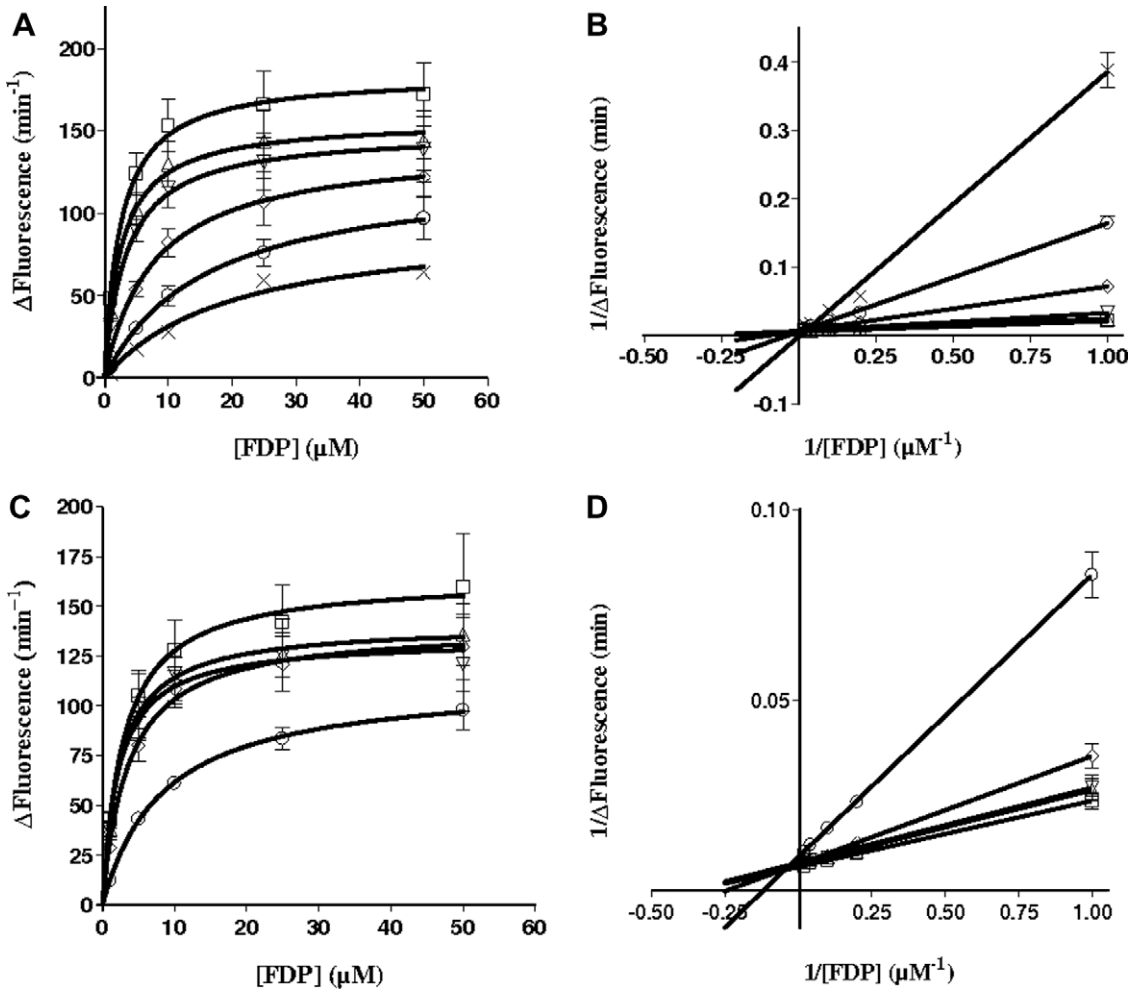

Figure 2. Kinetic analyses of CDC25B inhibition by compounds **4** and **6**. Concentrations of compound **4**: (□) 0 μM; (Δ) 0.3 μM; (▽) 1 μM; (◇) 3 μM; (o) 6 μM; (×) 10 μM. Concentrations of compound **6**: (□) 0 μM; (Δ) 0.3 μM; (▽) 1 μM; (◇) 3 μM; (o) 6 μM. (A) Michaelis-Menten plot of CDC25B inhibition by **4**. (B) Lineweaver–Burk plot of CDC25B inhibition by **4**. (C) Michaelis–Menten plot of CDC25B inhibition by **6**. (D) Lineweaver–Burk plot of CDC25B inhibition by **6**.

Table 2
Effect of DTT on in vitro CDC25B inhibition by compounds **4** and **6**.

Compound	% Inhibition at 100 μM[a]	
	DTT (10 mM)	DTT (20 mM)
4	42.45 ± 0.05	65.79 ± 2.70
6	51.63 ± 0.31	73.45 ± 1.72

[a] The % of inhibition were calculated from two independent experiments with three determinations per tested concentration.

compound **1e** did not show significant cytotoxicity with an IC_{50} value of 210 μM versus 37.7 μM for compound **2e**. Thus, in this series, a correlation between the in vitro enzymatic activity of the compounds and their cytotoxic effects on HeLa cell line was observed. Furthermore and as expected, the di-benzyl malonates **1c** and **2c** synthesized in order to improve cell penetration were more efficient than their acid analogs **1e** and **2e**. Surprisingly, compound **3** containing one carboxylic group was less active than its malonic acid analog **2e** with IC_{50} values of 54.2 and 37.7 μM, respectively.

Concerning the monoacid derivatives, the presence of a sulfur or a carbon atom had no effect on the cytotoxic properties since compounds **3** and **4** exhibited comparable efficiencies with IC_{50} values of 51.3 and 54.2 μM, respectively. Thus, compound **3** triggers targets other than CDC25 phosphatase in HeLa cells.

The 6,7-dibromoquinolinedione **5** showed moderate cytotoxic activity with an IC_{50} value of 21.5 μM. Quinolinedione derivative **6** with anti-phosphatase activity did not display potent cytotoxic activity on HeLa cells with an IC_{50} value above 100 μM as observed for its naphthoquinone analog.[29] Compound **7** with increased side chain lengths did not either show cytotoxicity. For these two compounds, the presence of the two carboxylic groups may impede cell penetration.

The antiproliferative effects of malonic acid **2e** were also examined on HeLa cells using a colony formation assay. HeLa cells were treated with increasing concentrations of **2e** and plated for ten additional days. After crystal violet staining and colony counting, the dose-response curve was drawn and the IC_{50} value determined. Compound **2e** was able to inhibit colony formation with an IC_{50} value of 3.3 μM and was more potent than Cpd 5 and NSC 95397, which displayed IC_{50} values of 4.1 and 8.5 μM, respectively in the same conditions.[29]

3.3. Effects on cell cycle progression

The effects of vitamin K_3 analogues and especially of Cpd 5 on cell cycle progression were previously examined on different tumor cell lines.[21,38,39] Studies carried out on asynchronous human hepatoma Hep3B cells showed that Cpd 5 was able to arrest cell cycle progression at the G2/M and G1 steps.[38] Similar results were

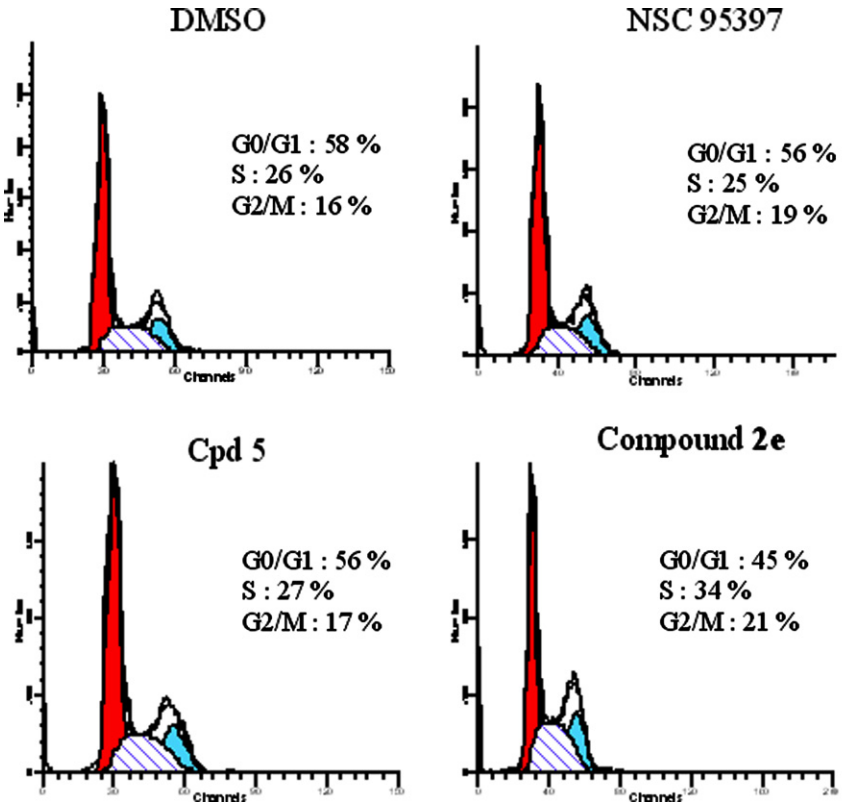

Figure 3. Cpd 5, NSC 95397, and naphthoquinone **2e** hardly modify cell cycle distribution. Asynchronous HeLa cells were treated with Cpd 5 and NSC95397 at a concentration of 10 μM and with compound **2e** at a concentration of 50 μM for 24 h and then stained for flow cytometry analysis. The cell distribution reported in each figure was measured as the percentage of cells containing DNA of G0/G1, S, and G2/M phases.

obtained on synchronous murine tsFT210 cells.[21] More recently, Han et al. demonstrated that Cpd 5 slightly modified cell cycle distribution of HCT-116 cell line at a concentration of 7.5 μM, whereas it appeared more efficient on HCT-116R30A as it arrested cell cycle at the G2/M transition at the same concentration. In this study, the authors also demonstrated that NSC 95397 was equally efficient on both cell lines and blocked cell cycle progression at the G2/M phase.[39]

The effects of Cpd 5, NSC 95397, and compound **2e** were examined in this study on cell cycle distribution using flow cytometry analysis on asynchronous HeLa cells (Fig. 3).

After 24 h treatment at a concentration of 10 μM of Cpd 5 and NSC 95397, cell cycle distribution hardly changed. In the presence of the reference compounds, cells were arrested at various stages of cell cycle progression suggesting that the activity of the three CDC25 isoforms was inhibited. Concerning compound **2e**, only a slight accumulation in the G2/M and S phases was observed at a concentration of 50 μM that may also be correlated with a decrease of CDC25 activity.

4. Conclusion

We have reported the synthesis and the CDC25 phosphatase inhibitory activity of novel naphthoquinone and quinolinedione derivatives. These compounds were designed to increase the interaction with the arginine residues involved in the recognition of the CDKs upon introducing malonic or acid groups at the extremity of an alkyl or a thio-alkyl side chain. Although these compounds did not show the expected increase of activity with IC_{50} value for the most potent one in the 10 μM range, they displayed moderate cytotoxicities against HeLa cell line. Interestingly, compound **2e** exhibited antiproliferative properties against HeLa cells and moderate effects on cell cycle distribution in accordance with CDC25 inhibitory effects. Further chemical investigation carried out on these derivatives could lead to new promising potent CDC25 inhibitors.

5. Experimental

5.1. Abbreviations

DBU, 1,8-diazabicyclo[5.4.0]undec-7-ene; DMF, dimethylformamide; DMSO, dimethylsulfoxide; THF, tetrahydrofuran; TMS, tetramethylsilane.

5.2. Chemicals

The intermediate 2-(2-naphthyl)ethyl bromide **2**[30] as well as Cpd 5,[21] NSC 95397,[34] 6,7-dibromoquinolinedione **5**[33], and 4-[3-methyl-(1,4-dioxo-1,4-dihydronaphthalen-2-yl)]butanoic acid **3**[32] were synthesized as previously reported. All other chemicals were purchased from Acros Organics and Aldrich and used without further purification unless otherwise specified.

5.3. General

All melting points were determined on a Kofler apparatus and are uncorrected. Kieselgel $60F_{254}$ plates (Merck) were used for analytical thin layer chromatography and were visualized with ultraviolet light (254 nm). Flash chromatography was performed on silica gel 60 (0.04–0.063 mm) purchased from Carlo Erba—SDS. ^{1}H and ^{13}C NMR spectra were recorded on a Bruker WMFT-250 MHz spectrometer. Chemical shifts were expressed in parts per million (ppm) using TMS as internal standard. Mass spectra

were recorded on a LCQ Advantage spectrometer (ThermoElectron, France) at the Laboratoire de Chimie et Biochimie Pharmacologiques et Toxicologiques, Université Paris Descartes, Paris, France. Elemental analyses (C, H, N), performed at the Service de Microanalyse, Pierre et Marie Curie Université, Paris, France, were within ±0.4% of the theoretical values.

5.4. General procedure for the synthesis of compounds (1a, 1b) and (2a, 2b)

A solution of diterbutyl or dibenzyl malonate (1 mmol) in dry DMF (10 mL) was added dropwise to a chilled suspension of NaH (1.1 mmol) in DMF (5 mL). The reaction mixture was stirred at 0 °C for an hour before a solution of 2-bromomethylnaphthalene or 2-(2-naphthyl)ethyl bromide **2** (1.1 mmol) dissolved in DMF (10 mL) was added dropwise. The resulting mixture was stirred at room temperature for 12 h and then diluted into water. The aqueous phase was extracted with ethyl acetate (3×). The organic layers were then washed with water and saturated aqueous NaCl, dried (Na_2SO_4), and evaporated to dryness. The residue was purified on silica gel column chromatography (EtOAc/cyclohexane, 1:9) to give the expected malonate derivatives **1a,b**–**2a,b**.

5.5. Dibenzyl (2-naphthylmethyl)malonate (1a)

Compound **1a** was obtained from 2-bromomethylnaphthalene (3 g, 13.57 mmol) and dibenzyl malonate (3.73 mL, 14.9 mmol) as a colorless oil (5.12 g, 89%); ^{1}H NMR ($CDCl_3$): δ 3.4 (t, 2H, J = 7.8 Hz, C*H*$_2$-CH), 3.88 (t, 1H, CH$_2$-C*H*), 5.09 (s, 4H, 2× CH$_2$ benzyl), 7.15–7.30 (m, 10H, Har), 7.42–7.46 (m, 2H, Har), 7.59 (s, 1H, Har), 7.65–7.88 (m, 4H, Har). ^{13}C NMR ($CDCl_3$): δ 35.35, 54.24, 67.66 (2C), 126.10, 126.51, 127.47, 127.96, 128.06, 128.14, 128.55 (5C), 128.73 (2C), 128.93 (5C), 132.86, 133.94, 135.51, 135.66, 168.98 (2C).

5.6. Diterbutyl (2-naphthylmethyl)malonate (1b)

Compound **1b** was obtained from 2-bromomethylnaphthalene (3 g, 13.57 mmol) and diterbutyl malonate (3.33 mL, 14.9 mmol) as a colorless oil (4.10 g, 85%); ^{1}H NMR ($CDCl_3$): δ 1.38 (s, 18H, 2× ^{t}Bu), 3.28 (d, 2H, J = 7.8 Hz, CH$_2$), 3.54 (t, 1H, CH), 7.31–7.34 (m, 1H, Har), 7.39–7.43 (m, 2H, Har), 7.64 (m, 1H, Har), 7.72–7.77 (m, 3H, Har). ^{13}C NMR ($CDCl_3$): δ 26.46 (6C), 33.35, 54.20, 80.21 (2C), 124.03, 124.56, 125.95, 125.99, 126.14, 126.21, 126.59, 130.90, 132.09, 134.53, 166.90 (2C).

5.7. Dibenzyl [2-(2-naphthyl)ethyl]malonate (2a)

Compound **2a** was obtained from 2-(2-naphthyl)ethyl bromide **2** (0.6 g, 2.55 mmol) and dibenzyl malonate (0.7 mL, 2.8 mmol) as a white powder (0.89 g, 80%); mp 75 °C; ^{1}H NMR ($CDCl_3$): δ *2.29–2.36* (m, 2H, CH$_2$–C*H*$_2$–CH), 2.78 (t, 2H, J = 7.6 Hz, C*H*$_2$–CH$_2$–CH), 3.47 (t, 1H, CH), 5.13 (s, 4H, 2× CH$_2$ benzyl), 7.30 (s, 10H, Har), 7.40–7.51 (m, 3H, Har), 7.68–7.79 (m, 4H, Har). ^{13}C NMR ($CDCl_3$): δ 30.62, 33.77, 51.64, 67.56 (2C), 125.77, 126.40, 127.23, 127.51, 127.89, 128.01, 128.65 (5C), 128.79 (2C), 128.99 (5C), 132.56, 133.95, 135.78, 138.31, 169.42 (2C).

5.8. Diterbutyl [2-(2-(naphthyl)ethyl]malonate (2b)

Compound **2b** was obtained from 2-(2-naphthyl)ethyl bromide **2** (1.5 g, 6.38 mmol) and diterbutyl malonate (1.57 mL, 7 mmol) as a white powder (2 g, 85%); mp 81 °C; ^{1}H NMR ($CDCl_3$): δ 1.46 (s, 18H, 2× ^{t}Bu), 2.18–2.21 (m, 2H, CH$_2$–C*H*$_2$–CH), 2.80 (t, 2H, J = 7.4 Hz, C*H*$_2$–CH$_2$–CH), 3.15–3.17 (m, 1H, CH), 7.31–7.34 (m, 1H, H$_3$), 7.42–7.43 (m, 2H, Har), 7.62 (m, 1H, Har), 7.74–7.80 (m, 3H, Har). ^{13}C NMR ($CDCl_3$): δ 28.32 (6C), 29.75, 30.54, 54.59, 80.46 (2C), 124.56, 124.96, 126.02, 126.09, 126.32, 126.45, 126.68, 131.54, 132.68, 135.06, 167.65 (2C).

5.9. General procedure for the preparation of compounds (1c, 1d) and (2c, 2d)

Periodic acid (4.2 mmol) was dissolved in acetonitrile (12 mL) under vigorous stirring and CrO_3 (0.1 mmol) was added. The solution was cooled to 5 °C and a solution of the previously synthesized naphthalene derivatives **1a,b**–**2a,b** (1 mmol) dissolved in acetonitrile (5 mL) was added. The resulting mixture was stirred at room temperature for 30 min and the precipitate filtered. The filtrate was evaporated under reduced pressure and the residue dissolved in a mixture of CH_2Cl_2/H_2O. The aqueous layer was extracted with dichloromethane. The organic layers were then washed with a solution of saturated aqueous NaCl, dried (Na_2SO_4), and the solvent removed under reduced pressure. The residue was finally purified on silica gel column chromatography (EtOAc/cyclohexane, 1:9) to give the expected naphthoquinones **1c,d**–**2c,d**.

5.10. Dibenzyl [(1,4-dioxo-1,4-dihydronaphthalen-2-yl)methyl] malonate (1c)

Compound **1c** was obtained from compound **1a** (1 g, 2.36 mmol) as a yellow powder (0.15 g, 28%); mp 72 °C; ^{1}H NMR ($CDCl_3$): δ 3.19 (d, 2H, J = 7.8 Hz, CH$_2$), 3.97 (t, 1H, CH), 5.16 (s, 4H, 2× CH$_2$ benzyl), 6.77 (s, 1H, H$_3$), 7.25–7.45 (m, 10H, Har), 7.74–7.77 (m, 2H, H$_6$ and H$_7$), 8.03–8.10 (m, 2H, H$_5$ and H$_6$); ^{13}C NMR (DMSO-d_6): δ 28.44, 49.96, 67.11 (2C), 125.99, 126.58, 128.24 (5C), 128.49 (2C), 128.71 (5C), 131.81, 134.53, 135.68 (2C), 136.39, 147.33, 168.29 (2C), 184.63 (2C); MS (ESI) m/z 477 (M+Na)$^+$. Anal. Calcd for $C_{28}H_{22}O_6$: C, 74.00; H, 4.88. Found: C, 73.83; H, 5.03.

5.11. Diterbutyl [(1,4-dioxo-1,4-dihydronaphthalen-2-yl)methyl] malonate (1d)

Compound **1d** was obtained from compound **1b** (0.5 g, 1.4 mmol) as a yellow powder (0.18 g, 37%); mp 120 °C; ^{1}H NMR ($CDCl_3$): δ 1.41 (s, 18H, 2× ^{t}Bu), 3.05 (d, 2H, J = 7.8 Hz, CH$_2$), 3.58 (t, 1H, CH), 6.81 (s, 1H, Har), 7.70–7.74 (m, 2H, H$_6$ and H$_7$), 8.02–8.09 (m, 2H, H$_5$ and H$_6$). ^{13}C NMR ($CDCl_3$): δ 28.28 (6C), 29.65, 52.58, 82.52 (2C), 126.52, 127.05, 132.40, 132.54, 134.18 (2C), 136.78, 148.39, 167.99 (2C), 185.06 (2C).

5.12. Dibenzyl [2-(1,4-dioxo-1,4-dihydronaphthalen-2-yl)ethyl] malonate (2c)

Compound **2c** was obtained from compound **2a** (0.3 g, 0.68 mmol) as a yellow oil (50 mg, 15%); ^{1}H NMR ($CDCl_3$): 2.21–2.30 (m, 2H, CH$_2$–C*H*$_2$–CH), 2.64 (t, 2H, J = 7.5 Hz, C*H*$_2$–CH$_2$–CH), 3.56 (t, 1H, J = 7.4 Hz, CH), 5.18 (s, 4H, 2× CH$_2$ benzyl), 6.78 (s, 1H, H$_3$), 7.35 (m, 10H, Har),7.74–7.78 (m, 2H, H$_6$ and H$_7$), 8.07–8.13 (m, 2H, H$_5$ and H$_6$); ^{13}C NMR (DMSO-d_6): δ 26.99, 27.02, 50.82, 66.90 (2C), 125.88, 126.50, 128.27 (5C), 128.52 (2C), 128.79 (5C), 132.00, 132.27, 134.36, 135.46, 135.86, 150.02, 168.93 (2C), 184.9 (2C); MS (ESI) m/z 491 (M+Na)$^+$. Anal. Calcd for $C_{29}H_{24}O_6$: C, 74.35; H, 5.16. Found: C, 74.23; H, 5.12.

5.13. Diterbutyl [2-(1,4-dioxo-1,4-dihydronaphthalen-2-yl)ethyl] malonate (2d)

Compound **2d** was obtained from compound **2b** (1.3 g, 3.51 mmol) as a yellow oil (150 mg, 39%); ^{1}H NMR ($CDCl_3$): δ 1.45 (s, 18H, 2× ^{t}Bu), 2.06–2.12 (m, 2H, CH$_2$–C*H*$_2$–CH), 2.61 (t,

2H, J = 7.4 Hz, CH_2CH_2CH), 3.19 (t, 1H, J = 7.8 Hz, CH), 6.81 (s, 1H, H_3), 7.69–7.73 (m, 2H, H_6 and H_7), 8.03–8.08 (m, 2H, H_5 and H_6). ^{13}C NMR ($CDCl_3$): δ 27.30, 27.69, 28.29 (6C), 53.71, 82.14 (2C), 126.44, 127.01, 132.47, 132.63, 134.06 (2C), 135.63, 150.85, 168.66 (2C), 185.20, 185.33.

5.14. General procedure for the preparation of malonic acids 1e and 2e

Trifluoroacetic acid (0.3 mL) was added to a solution of diterbutyl malonate **1d** or **2d** (0.3 mmol) dissolved in dichloromethane (10 mL). The reaction mixture was then stirred at room temperature for 12 h. The solvent was removed under reduced pressure and the residue was taken up in ether. Finally, the precipitate was filtered to give the expected acids **1e** and **2e**.

5.15. [(1,4-Dioxo-1,4-dihydronaphthalen-2-yl)methyl]malonic acid (1e)

Compound **1e** was obtained from compound **1d** (140 mg, 0.36 mmol) as a yellow powder (45 mg, 70%); mp 212 °C; ^{1}H NMR ($CDCl_3$): δ 3.02-3.05 (d, 2H, J = 7.4 Hz, CH_2), 3.71 (t, 1H, CH), 6.96 (s, 1H, H_3), 7.91–7.95 (m, 2H, H_6 and H_7), 8.03–8.11 (m, 2H, H_5 and H_6); ^{13}C NMR (DMSO-d_6): δ 28.69, 50.52, 126.00, 126.61, 131.81, 132.06, 134.57, 135.85, 135.88, 148.43, 170.31 (2C), 184.63, 184.81; MS (ESI) m/z 273 $(M+H)^+$. Anal. Calcd for $C_{14}H_{10}O_6{\cdot}0.5H_2O$: C, 59.36; H, 3.88. Found: C, 59.28; H, 3.94.

5.16. [2-(1,4-Dioxo-1,4-dihydronaphthalen-2-yl)ethyl]malonic acid (2e)

Compound **2e** was obtained from compound **2d** (0.13 g, 0.33 mmol) as a gray powder (78 mg, 82%); mp 238 °C; ^{1}H NMR ($CDCl_3$): δ *2.04–2.10* (m, 2H, CH_2–CH_2–CH), 2.56 (t, 2H, J = 7.4 Hz, CH_2–CH_2–CH), 3.30 (m, 1H, CH), 6.84 (s, 1H, H_3), 7.90–7.96 (m, 2H, H_6 and H_7), 8.02–8.10 (m, 2H, H_5 and H_6); ^{13}C NMR (DMSO-d_6): δ 26.82, 27.33, 51.41, 125.89, 126.50, 132.01, 132.30, 134.35, 135.17, 135.21, 150.44, 170.98 (2C), 184.84, 184.89; MS (ESI) m/z 287 $(M+H)^+$. Anal. Calcd for $C_{15}H_{12}O_6{\cdot}0.5H_2O$: C, 60.60; H, 4.20. Found: C, 60.18; H, 4.21.

5.17. 3-[(3-Methyl-1,4-dioxo-1,4-dihydronaphthalen-2-yl)sulfanyl]propanoic acid (4)

Compound **4** was obtained according to reported procedure[21] from menadione (1 g, 8.71 mmol) and mercaptopropanoic acid (0.5 ml, 8.71 mmol) as an orange powder (470 mg, 20%); mp 163 °C; ^{1}H NMR (DMSO-d_6): δ 2.26 (s, 3H, CH_3), 2.61 (t, 2H, J = 6.7 Hz, S–CH_2), 3.30 (t, 2H, CH_2–CO_2H), 7.83–7.86 (m, 2H, H_6 and H_7), 8.00–8.04 (m, 2H, H_5 and H_6); ^{13}C NMR (DMSO-d_6): δ 15.99, 29.86, 36.14, 126.88, 127.27, 132.43, 133.37, 134.55, 134.75, 147.56, 173.64, 181.42, 182.55; MS (ESI) m/z 275 $(M-H)^-$. Anal. Calcd for $C_{14}H_{12}O_4S$: C, 60.87; H, 4.34. Found: C, 61.60; H, 4.40.

5.18. General procedure for the preparation of quinolinediones (6) and (7)

To a solution of 6,7-dibromo-5,8-quinolinedione **5** (1 mmol) dissolved in THF (6 mL) were added mercaptoacetic acid or mercaptopropanoic acid (2.5 mmol) and triethylamine (3 mmol). The reaction mixture was stirred at room temperature for 2 h and then poured into water. The precipitate was filtered to give the expected quinolinediones **6** and **7**.

5.19. 2,2′-[(5,8-Dioxo-5,8-dihydroquinoline-6,7-diyl)disulfanediyl] diacetic acid (6)

Compound **6** was obtained from 6,7-dibromo-5,8-quinolinedione **5** (400 mg, 1.26 mmol) and mercaptoacetic acid (0.22 mL, 3.8 mmol) as a yellow powder (141 mg, 33%); mp 195 °C; ^{1}H NMR (CD_3OD): δ 3.78 (s, 2H, CH_2), 3.90 (s, 2H, CH_2), 7.57 (dd, 1H, J = 4.4 Hz, J = 8.4 Hz, H_6), 8.62 (d, 1H, H_7), 8.87 (d, 1H, H_5); ^{13}C NMR (DMSO-d_6): δ 35.66, 38.20, 116.04, 119.46, 120.00, 122.17, 132.27, 139.08, 147.52, 147.72, 150.13, 171.27, 172.44; MS (ESI) m/z 342 $(M+2H)^+$. Anal. Calcd for $C_{13}H_9NO_6S{\cdot}0.5H_2O$: C, 44.78; H, 2.87; N, 4.02. Found: C, 44.58; H, 2.93; N, 3.97.

5.20. 3,3′-[(5,8-Dioxo-5,8-dihydroquinoline-6,7-diyl)disulfanediyl] dipropanoic acid (7)

Compound **7** was obtained from 6,7-dibromo-5,8-quinolinedione **5** (400 mg, 1.26 mmol) and mercaptopropanoic acid (0.28 mL, 3.8 mmol) as a red powder (291 mg, 63%); mp 205 °C; ^{1}H NMR (CD_3OD): δ 2.70 (s, 4H, 2× CH_2), 3.50 (s, 4H, 2× CH_2), 7.80 (dd, 1H, J = 4.4 Hz, J = 8.4 Hz, H_6), 8.48 (d, 1H, H_7), 8.90 (d, 1H, H_5); ^{13}C NMR (DMSO-d_6): δ 30.29, 35.97 (2 C), 45.81, 128.59, 130.76, 135.35, 149.40, 154.67, 173.72 (4 C), 177.92, 179.19; MS (ESI) m/z 366 $(M-H)^-$. Anal. Calcd for $C_{15}H_{13}NO_6S_2$: C, 47.87; H, 3.72; N, 3.72. Found: C, 48.05; H, 3.78; N, 4.18.

5.21. Enzyme, cell culture, chemicals, and antibodies

The recombinant MBP-CDC25B3 protein was produced in bacteria as previously described.[40] Human cancer cell line HeLa was obtained from Aptanomics (Lyon, France). Cells were cultured at 37 °C in Dulbecco's minimum essential medium complemented with 10% fetal bovine serum and 100 U/ml penicillin/streptomycin in a humidified atmosphere of 5% CO_2. The tetrazolium salt WST-1 was purchased from Roche Diagnostics (Mannheim, Germany) and propidium iodide from Sigma–Aldrich (St Louis, MO, USA). The following antibodies were used for flow cytometry analysis: anti-H3P antibody from Upstate Biotechnology (Lake Placid, NY, USA) and anti-rabbit Alexa 488 antibody from Sigma-Aldrich (St Louis, MO, USA).

5.22. In vitro enzymatic assay and Steady-State Kinetics

The activity of the MBP-CDC25B3 recombinant enzyme was monitored using fluorescein diphosphate. The assay was performed in 96-well plates in a final volume of 200 μL. MBP-CDC25B3 was diluted in assay buffer [30 mM Tris–HCl (pH 8.2), 75 mM NaCl, 0.67 mM EDTA, 0.033% BSA, 1 mM DTT] so that the final concentration was 90 ng/well. The reaction was initiated by addition of 30 μM of fluorescein diphosphate followed by immediate measurement of fluorescein monophosphate emission with a Fluoroskan Ascent (Lab Systems; excitation filter: 485 nm, emission filter: 530 nm). For each compound, the drug concentration required for 50% inhibition (IC_{50}) was determined from a sigmoidal dose-response curve using GraphPad Prism 4 (GraphPad Software, San Diego, CA). Compounds **4** and **6** were added to the wells at a final concentration of 0.3, 1, 3, 6 and 10 μM. Substrate concentration was varied between 1 and 50 μM (K_m = 2.89 μM). The results are expressed as the mean of two independent experiments with three determinations per tested concentration and per experiment.

5.23. Cell proliferation assay

The inhibition of cell proliferation was determined using a colorimetric assay based on the cleavage of the WST-1 tetrazolium salt by mitochondrial dehydrogenases in viable cells, leading to

formazan formation. On day 1, HeLa cells were plated at 3000 cells/well in 96-well culture plates with 95 μL of medium/well. On day 2, cells were treated for 96 h with 5 μL of increasing concentrations of drug. On day 6, after addition of 10 μL of WST-1 per well, cells were incubated for 2 h at 37 °C in a humidified atmosphere of 5% CO_2. Absorbance was measured at 430 nm. The results are expressed as the mean of three independent experiments with eight determinations per tested concentration and per experiment. For each compound, the IC_{50} value was determined from a sigmoidal dose-response using GraphPad Prism (GraphPad Software, San Diego, CA).

5.24. Clonogenic assay

For cloning inhibition assays, HeLa cells were plated at 100 cells/well in 6-well culture plates with 2.5 mL of medium/well. After 24 h growing at 37 °C in a humidified atmosphere of 5% CO_2, the culture medium was replaced by control medium or medium containing inhibitors at increasing concentrations (up to 100 μM) and incubated for 10 days. Cells were then washed with phosphate-buffered saline and fixed in 10% formaldehyde for 30 min at room temperature. They were carefully rinsed with water, stained with 1 mL crystal violet (2 g in 100 mL ethanol, then 2 mL in 100 mL water) for 10 min and finally rinsed with water. The plating efficiency was determined by counting the colonies. The results are expressed as the mean of three independent experiments. For each compound, the IC_{50} value was determined from a sigmoidal dose-response using GraphPad Prism (GraphPad Software, San Diego, CA).

5.25. Flow cytometry analysis

The analysis of cell cycle distribution by flow cytometry was conducted with asynchronous HeLa cells. After 24 h growing at 37 °C in a humidified atmosphere of 5% CO_2, cells were treated with 10 μM of Cpd 5 or NSC 95397 or 50 μM of compound **2e,** and were incubated for an additional 24 h. Cells were then detached by trypsin treatment, centrifugated, washed with PBS, and suspended in 50 μL of PBS. Cold 100% ethanol was carefully added and cells were incubated at −20 °C for an additional 2 h. After centrifugation at 215*g* for 4 min, cells were washed with a PBS solution containing 1% BSA and subjected to an additional centrifugation at 215*g* for 4 min. They were then suspended in a solution of 0.25% Triton 100× in PBS 1X, incubated at 4 °C for 15 min, centrifugated, washed with PBS containing 1% BSA, and treated with 30 μL of anti-H3 P antibody. After 1h30 of incubation at room temperature, 1 mL of 1% BSA PBS solution was added. Cells were centrifugated at 215*g* for 4 min, resuspended in PBS containing 1% BSA, subjected to an additional centrifugation and treated with monoclonal anti-rabbit Alexa antibody at 1:8000 dilution. After 45 min incubation at room temperature in the dark, cells were washed with 1% BSA PBS, subjected to centrifugation at 215*g* for 4 min and, resuspended in a 1× PBS solution containing 1 μg/mL of RNase. Propidium iodide (10 μg/mL) was added to the medium, and cells were incubated at 37 °C in the dark for 30 min and finally analyzed with a BD FACSCalibur flow cytometer (BD Biosciences, San Jose, CA, USA). Each CDC25 inhibitor was analyzed three independent times. Cells treated with DMSO served as negative control.

5.26. Molecular modeling

The available crystal structure of the catalytic subunit of CDC25B (PDB code 1QB0) was used to dock compound **1e**. Molecular dynamics calculations were carried out using Discover (Accelrys). Inhibitors were built using the program Builder (Accelrys) and the cff91force field. Energy minimizations and molecular dynamics were realized without considering water molecules and by fixing the value of the dielectric constant to 4. The protein backbone was held frozen, while the lateral chains and the inhibitor were relaxed. After 5000-fs initialization at 300 K, 100 steps of molecular dynamics calculations were performed. Each was done at 300 K during 5000 steps of 1 fs. As in Ref. [41], the resulting conformations were submitted to a conjugate-gradient energy minimization and stored.

Acknowledgments

We are grateful to Dr. Wang-Qing Liu for mass spectra recording. This research is supported by La Ligue Nationale contre le Cancer, Equipe Labellisée 2006 (U648) and Equipe Labellisée 2008 (UMR 5088-IFR109).

References and notes

1. Strausfeld, U.; Labbe, J. C.; Fesquet, D.; Cavadore, J. C.; Picard, A.; Sahdu, K.; Russell, P.; Doree, M. *Nature* **1991**, *351*, 242.
2. Honda, R.; Ohba, Y.; Nagata, A.; Okayama, H.; Yasuda, H. *FEBS Lett.* **1993**, *318*, 331.
3. Galaktionov, K.; Beach, D. *Cell* **1991**, *67*, 1181.
4. Sadhu, K.; Reed, S. I.; Richardson, H.; Russell, P. *Proc. Natl. Acad. Sci. U.S.A.* **1990**, *87*, 5139.
5. Nagata, A.; Igarashi, M.; Jinno, S.; Suto, K.; Okayama, H. *New Biol.* **1991**, *3*, 959.
6. Hoffmann, I.; Draetta, G. F.; Karsentti, E. *EMBO J.* **1994**, *13*, 4302.
7. Jinno, S.; Suto, J.; Nagata, A.; Igarashi, M.; Kanaoka, Y.; Nojima, H.; Okayama, H. *EMBO J.* **1994**, *13*, 1549.
8. Molinari, M.; Mercurilo, C.; Dominguez, J.; Goubin, F.; Draetta, G. F. *EMBO Rep.* **2000**, *1*, 71.
9. Boutros, R.; Lobjois, V.; Ducommun, B. *Nat. Rev. Cancer* **2007**, *7*, 495.
10. Lammer, C.; Wagerer, S.; Saffrich, R.; Mertens, D.; Ansorge, W.; Hoffmann, I. *J. Cell Sci.* **1998**, *111*, 2445.
11. Boutros, R.; Lobjois, V.; Ducommun, B. *Cancer Res.* **2007**, *67*, 11557.
12. Garner-Hamrick, P. A.; Fischer, C. *Int. J. Cancer* **1998**, *76*, 720.
13. Van Vugt, M. A. T. M.; Bras, A.; Medema, R. H. *Mol. Cell* **2004**, *15*, 799.
14. Bugler, B.; Quaranta, M.; Aressy, B.; Brezak, M. C.; Prevost, G.; Ducommun, B. *Mol. Cancer Ther.* **2006**, *5*, 1446.
15. Millar, J. B.; Blewitt, J.; Gerace, L.; Sadku, K.; Featherstone, C.; Russell, P. *Proc. Natl. Acad. Sci. U.S.A.* **1991**, *88*, 10500.
16. Turowski, P.; Franckhauser, C.; Morris, M. C.; Vaglio, P.; Fernandez, A.; Lamb, N. J. *Mol. Biol. Cell* **2003**, *14*, 2984.
17. Kristjandottir, K.; Rudolph, J. *Chem. Biol.* **2004**, *11*, 1043.
18. Galaktionov, K.; Lee, A. K.; Eckstein, J.; Draetta, G. F.; Meckler, J.; Loda, M.; Beach, D. *Science* **1995**, *269*, 1575.
19. Contour-Galcera, M. O.; Sidhu, A.; Prévost, G.; Bigg, D.; Ducommun, B. *Pharmacol. Therap.* **2007**, *115*, 1.
20. Nishikawa, Y.; Carr, B. I.; Wang, M.; Kar, S.; Finn, F.; Dowd, P.; Zheng, Z. B.; Kerns, J.; Naganathan, S. *J. Biol. Chem.* **1995**, *270*, 28304.
21. Tamura, K.; Southwick, E. C.; Kerns, J.; Rosi, K.; Carr, B. I.; Wilcox, C.; Lazo, J. S. *Cancer Res.* **2000**, *60*, 1317.
22. Lazo, J. S.; Nemoto, K.; Pestell, K. E.; Cooley, K. A.; Southwick, E. C.; Mitchell, D. A.; Furey, W.; Gussio, R.; Zaharevitz, D. W.; Joo, B.; Wipf, P. *Mol. Pharmacol.* **2002**, *61*, 720.
23. Lazo, J. S.; Aslan, D. C.; Southwick, E. C.; Cooley, K. A.; Ducruet, A. P.; Joo, B.; Vogt, A.; Wipf, P. *J. Med. Chem.* **2001**, *44*, 4042.
24. Pu, L.; Amoscato, A. A.; Bier, M. E.; Lazo, J. S. *J. Biol. Chem.* **2002**, *277*, 46877.
25. Cao, S.; Forster, C.; Brisson, M.; Lazo, J. S.; Kingston, D. G. I. *Bioorg. Med. Chem.* **2005**, *13*, 999.
26. Brezak, M. C.; Quaranta, M.; Contour-Galcera, M. O.; Lavergne, O.; Mondesert, O.; Auvray, P.; Kasprzyk, P. G.; Prevost, G.; Ducommun, B. *Mol. Cancer Ther.* **2005**, *4*, 1378.
27. Cazales, M.; Boutros, R.; Brezak, M. C.; Chaumeron, S.; Prévost, G.; Ducommun, B. *Mol. Cancer Ther.* **2007**, *6*, 1.
28. Galcera-Contour, M. O.; Bigg, D.; Prevost G.; Sidhu D. Patent WO 2006/067311.
29. Brun, M. P.; Braud, E.; Angotti, D.; Mondesert, O.; Montes, M.; Miteva, M.; Gresh, N.; Ducommun, B.; Garbay, C. *Bioorg. Med. Chem.* **2005**, *13*, 4871.
30. Campaigne, E.; Heaton, B. G. *J. Org. Chem.* **1964**, *29*, 2372.
31. Yamazaki, S. *Tetrahedron Lett.* **2001**, *42*, 3355.
32. Salmon-Chemin, L.; Buisine, E.; Yardley, V.; Kohler, S.; Debreu, M. A.; Landry, V.; Sergheraert, C.; Croft, S. L.; Luise Krauth-Siegel, R.; Davioud-Charvet, E. *J. Med. Chem.* **2001**, *44*, 548.
33. Ryu, C. K.; Kang, H. Y.; Lee, S. K.; Nam, K. A.; Hong, C. Y.; Ko, W. G.; Lee, B. H. *Bioorg. Med. Chem. Lett.* **1999**, *9*, 1075.
34. Kulka, M. *Can. J. Chem.* **1962**, *40*, 1235.

35. Peng, H.; Xie, W.; Otterness, D. M.; Cogswell, J. P.; McConnell, R. T.; Carter, H. L.; Powis, G.; Abraham, R. T.; Zalkow, L. H. *J. Med. Chem.* **2001**, *44*, 834.
36. Brault, L.; Denancé, M.; Banaszak, E.; El Maadidi, S.; Battaglia, E.; Bagrel, D.; Samadi, M. *Eur. J. Med. Chem.* **2007**, *42*, 243.
37. Cossy, J.; Belotti, D.; Brisson, M.; Skoko, J. J.; Wipf, P.; Lazo, J. S. *Bioorg. Med. Chem.* **2006**, *14*, 6283.
38. Wang, Z.; Southwick, E.; Wang, M. F.; Rosi, K.; Lazo, J. S.; Wilcox, C. S.; Carr, B. I. *Cancer Res.* **2001**, *61*, 7211.
39. Han, Y.; Shen, H.; Carr, B. I.; Wipf, P.; Lazo, J. S.; Pan, S. S. *J. Pharmacol. Exp. Ther.* **2004**, *309*, 64.
40. Brezak, M. C.; Quaranta, M.; Mondesert, O.; Galcera, M. O.; Lavergne, O.; Alby, F.; Cazales, M.; Baldin, V.; Thurieau, C.; Harnett, J.; Lanco, J.; Kasprzyk, P. G.; Prevost, G. P.; Ducommun, B. *Cancer Res.* **2004**, *64*, 3320.
41. Liu, W. Q.; Vidal, M.; Gresh, N.; Roques, B. P.; Garbay, C. *J. Med. Chem.* **1999**, *42*, 3737.